

Towards an optical lattice clock based on mercury: loading of a dipole trap

S.Mejri, J.J McFerran, L. Yi, and S. Bize

LNE-SYRTE, Observatoire de Paris, UMR CNRS 8630, UPMC, 61 avenue de l'Observatoire, 75014 Paris, France.

Email:sebastien.bize@obspm.fr

ABSTRACT

In the pursuit of developing an optical lattice clock with mercury as the quantum absorber, we describe an experiment that produces dipole lattice trapping of neutral mercury atoms. We report on the details of an optical lattice trap with light near the predicted magic wavelength and on the implementation of a low noise detection system.

INTRODUCTION

Ion based frequency references have been leading the way in terms of line-centre accuracy [1, 2]. Some neutral atom based clocks have the potential of reaching similar levels of accuracy with less integration time, due to the higher number of quantum absorbers [7]. With the range of atomic clocks being built this provides numerous tests for searching for possible drifts in fundamental constants [3, 4]. Optical lattice clocks using strontium atoms have demonstrated uncertainties at the 10^{-16} level [5]. The blackbody radiation shift is the largest correction and the largest contribution to the strontium clock uncertainty and it will pose a hard limitation at the 10^{-17} level [6]. In contrast, neutral mercury has been recognized as having a low sensitivity to blackbody radiation while retaining other desirable features for an optical lattice clock [7]. A mercury based clock has the potential to achieve uncertainty in the low 10^{-18} range [7].

In the last few years, we have completed several steps toward the realization of a mercury optical lattice clock. Magneto-optical trapping (MOT) has been performed on several of the mercury isotopes: ^{199}Hg , ^{200}Hg , ^{201}Hg and ^{202}Hg . The MOT is generated by the intersection of three orthogonal pairs of retro-reflected $\sigma+$, $-\sigma$ polarized laser beams with a diameter of $\sim 14\text{mm}$ and a power of approximately 6mW in each arm. The MOT uses the $254\text{ nm } ^1\text{S}_0 - ^3\text{P}_1$ intercombination transition with a linewidth $\Gamma/2\pi=1.3\text{MHz}$. External coils to the vacuum chamber generate the magnetic quadrupole field with a gradient of $\sim 0.10\text{mT/mm}$ along the coil axis. By using a 265.6 nm ultra-stable laser source described in [4, 5], the Doppler-free spectroscopy and the absolute frequency measurement of the clock transition were carried out using this MOT apparatus, which improves our knowledge of this transition by more 4 orders of magnitude for fermionic isotopes [6].

As a preparation step for dipole lattice trapping and in order to further characterize the MOT, we use an electron multiplying cooled CCD camera, and by manipulating one of the MOT arms we manage to capture the fluorescence along the same axis while simultaneously operating the MOT, as illustrated in Fig.1.

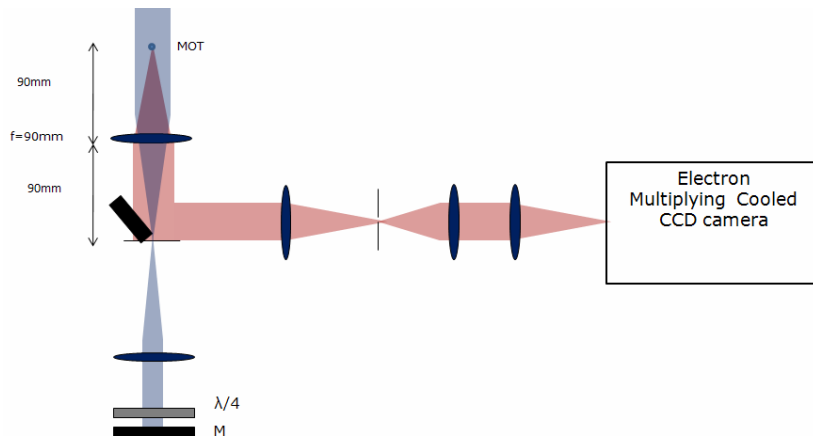


Fig.1. Schematic view of the MOT imaging system:
The MOT is imaged along the same axis as one of the MOT laser beam.

By observing the ballistic expansion of the MOT cloud, we are able to assess the temperature and determine the detuning frequency that leads to minimized temperatures. With 32mW of UV light in the six arms of the MOT, a minimum of 65 μ K was measured for the ^{202}Hg and ^{200}Hg bosons and temperatures of 45 μ K and 30 μ K were measured for the ^{199}Hg and ^{201}Hg fermionic isotopes respectively. The typical cloud size is 100 μ m and more than 2×10^6 ^{202}Hg atoms have been observed in the MOT. The corresponding density is greater than 10^{11}cm^{-3} which bodes well for loading atoms into the lattice trap. A detailed report of these finding will be published elsewhere.

IMPLEMENTATION OF A DIPOLE LATTICE AT THE MAGIC WAVELENGTH

The frequency of the $^1S_0 - ^3P_0$ clock transition in a lattice of depth U_0 is shifted with respect to the unperturbed frequency ν_0 by

$$\nu = \nu_0 + \nu_1 \frac{U_0}{E_R} \quad (1)$$

With ν_1 proportional to the dynamic polarizability difference between both states of the clock transition and E_R is the recoil energy corresponding to the photon atom recoil due to the lattice trap light defined by $E_R = \frac{\hbar^2 k_l^2}{2m}$.
 $k_l = \frac{2\pi}{\lambda_l}$ where λ_l is the wavelength of the lattice trap and m is the atomic mass.

By appropriately selecting the lattice light frequency such that the light-shift of the lower and upper levels become identical and we can have $\nu_1 \rightarrow 0$ [7]. In our experiment we use a dipole lattice trap at $\lambda_l = 362\text{ nm}$ which is one of the predicted magic wavelengths for mercury [3]. The corresponding recoil frequency in Hertz $E_R/(2\pi\hbar) = 7.7\text{ kHz}$. The flip side to the low blackbody radiation dependence of mercury is its low ground state polarizability. For example when we compare Hg to Sr for a trap depth of $1000E_R$ with a waist of 90 μ m, 9W is required for the lattice cavity power Sr and about 160W for Hg.

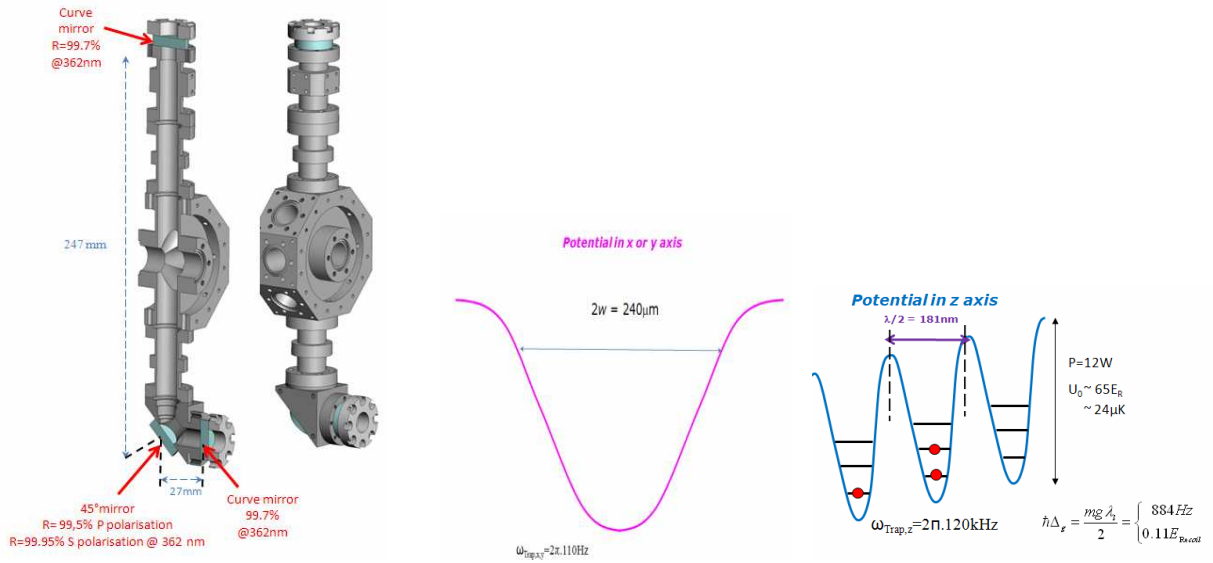


Fig. 2. Lattice cavity design and the lattice profile for mercury.

To generate the lattice light near the predicted magic wavelength, we use a CW titanium sapphire laser delivering about 900 mW at 724nm. This laser light is frequency doubled using an LBO crystal in a bow-tie resonant cavity. We generate up to 320mW at 362nm. The natural energy scale for describing the potential of the lattice trap is the recoil energy imposed on the Hg atom by the lattice trapping photons.

Using a parabolic approximation of the potential of the bottom of the trap, we find the longitudinal trap frequency satisfies:

$$\frac{1}{2} m \omega_z^2 z^2 \approx U_0 k_l^2 z^2 \quad (2)$$

which gives

$$\omega_z \approx \frac{4\pi^2 \hbar \sqrt{\frac{U_0}{E_R}}}{m \lambda_l^2} \quad (3)$$

From the oscillation frequency along the longitudinal axis we can calculate the oscillation frequency in the transverse plane using the following expression:

$$\frac{\omega_z}{\omega_r} = \frac{\sqrt{2}}{k_l w} \quad (4)$$

where w is the waist of the trapping beam.

For the design of the lattice cavity, we targeted 12 W as the internal power and a trap waist of $120\mu\text{m}$ forming a trap depth of $65E_R$ correspond to $24\mu\text{K}$. The corresponding longitudinal trap frequency is 120 kHz and the transverse trap frequency 110Hz. An optical cavity resonant with the incoming light is maintained under vacuum in conjunction with the 3D MOT chamber. To attempt to achieve these targets, the design schematic, shown in Fig.2, avoids the use of windows thus permitting a high build up factor and reducing the level of the stray light from the optical cavity reaching the detection system.

Since the heating due to the amplitude fluctuations of the trap can limit the lifetime of the atoms in the trap, we have carefully measured and stabilized the intensity of the lattice light source. The heating due to amplitude variations of the trapping behaves as a parametric excitation of the atoms in a harmonic potential well. The expression for the heating rate due to amplitude variations in the trap [8] is given by the following expression:

$$\frac{d}{dt}\langle E \rangle = \gamma \langle E \rangle$$

$$\gamma = \pi^2 v_{tr}^2 S_E(2v_{tr}) \quad (5)$$

where the trap oscillation frequency v_{tr} is measured in hertz and S_E is the fractional intensity noise power spectral density.

In Fig. 3 we present the relative intensity noise of the lattice light for free running operation (blue curve) and for active intensity stabilization (black curve). For comparison, we show the curve that corresponds to a 1s lifetime of the trap (red curve), according to the above equation.

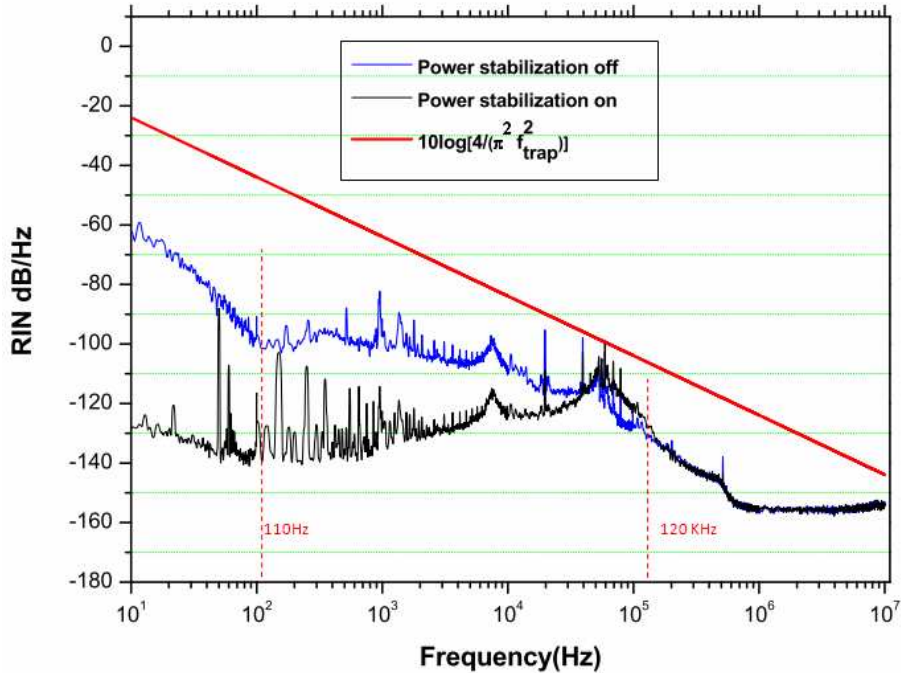


Fig.3. Relative intensity noise power spectral density of the lattice light.

From this we see that the low level of amplitude noise should permit lattice trapping lifetime of more than 1s. We note that the lifetime of the atoms in the MOT is $\sim 1.5\text{s}$ most likely limited by background collisions one therefore expects lattice trapping lifetime of this length in our system.

EXPECTED LOADED FRACTION AND DETECTIVITY

The estimated loaded fraction into the optical lattice from the MOT was calculated as a function of the internal power. Throughout the loading cycle, the lattice is overlapped with the MOT and cold atoms with energy smaller than the lattice depth remain trapped when the MOT light is switched off. A calculation of the fraction of atoms transferred from

the MOT to the lattice trap is shown in Fig. 4. Here we assume a waist size of $120\mu\text{m}$ for the lattice light, matching closely the rms size of the MOT cloud. At the anticipated power of 12W we expect a 0.35% transfer of atoms at $80\mu\text{K}$ (^{200}Hg , ^{202}Hg) and 1.4% for atoms at $30\mu\text{K}$ (^{201}Hg). Between 1W and 100W the dependence on power is proportional to $P^{1.3}$, while at 12W the fraction loaded is proportional to $T^{1.2}$.

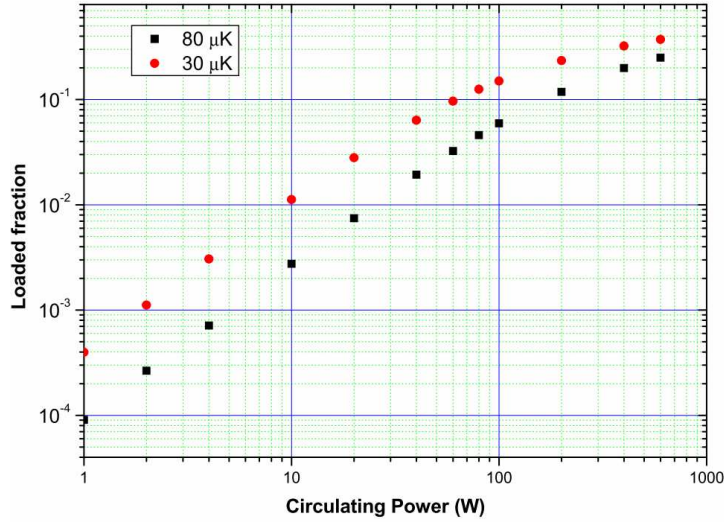


Fig.4. Calculated loaded fraction vs circulating power in the lattice cavity:
Red MOT temperature of $30\mu\text{K}$ and black temperature of $80\mu\text{K}$.

While making an initial attempting to load the lattice, a significant drop of the internal power of the lattice cavity was observed: 18W reduced to 3W within few minutes, tests with a similar cavity without vacuum showed little degradation of cavity power build up. The reason for the reduced finesse under vacuum is yet to be discovered. The reduced power led us to push the detectivity of our system; we have developed an efficient computed background subtraction algorithm that enhances the signal-to-noise ratio enabling detection of trapped atoms even with low internal power. In addition to that we used a 2×2 binning of the CCD array and that reduce the noise level by 40% . Two of the MOT beams are used for detecting at a detuning of -1Γ with exposure time of $\sim 2\text{ms}$.

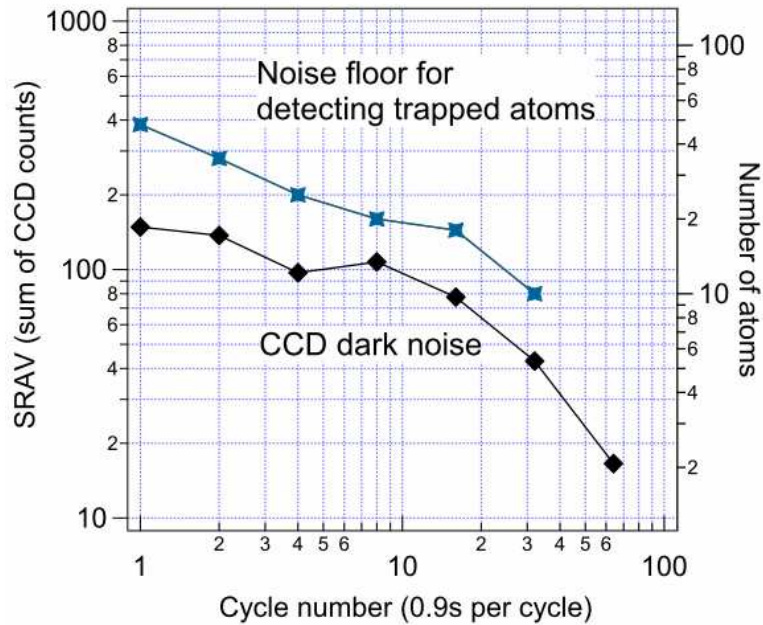


Fig.5. Allan standard deviation of CCD counts (left axis) and the corresponding number of atoms (right axis) vs cycle number.

We achieved a detection noise equivalent to ~ 40 atoms per shot as shown in Fig.5 which corresponds to less than 10^{-5} of the MOT signal. The noise level is approaching the readout noise of the CCD.

DIPOLE LATTICE TRAPPING OF NEUTRAL MERCURY

Operating with ~ 3 W in the lattice trap, and using the sequence shown in Fig.6, we have been able to detect lattice trapping of isotopes ^{199}Hg and ^{200}Hg .

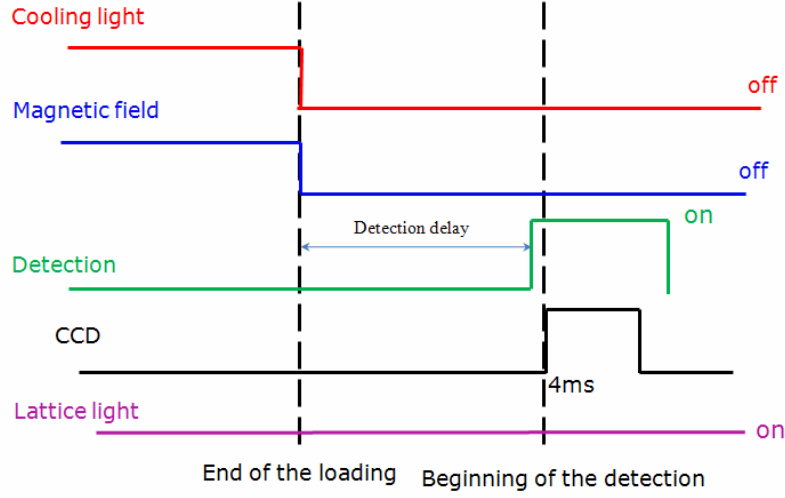


Fig. 6. Sequence for loading the lattice.

Because the probing of the lattice trapped atoms for detection removes atoms from the trap, there is a detection duration that optimizes the SNR of the lattice trapping signal. We find this duration to 4 ms under present circumstances.

By looking to the variation of the signal as a function of the detection delay (Fig.7) we show the lifetime of the trap to be 420ms and the number of atoms in the trap to be around ~ 300 atoms for ^{199}Hg . Similar measurements have been done for the ^{200}Hg showing a lifetime of ~ 230 ms. It's not clear why the lifetime are less than the expected 1s lifetime predicted by Fig.3. The different lifetime from one isotope to the other could be due to the different lattice light power in the two measurements. These issues need to be investigated.

In Fig.8 we show the cross section profile averaging over 18 frames of the dipole trapped atoms for a release time of 40 ms. This profile, confirms the fact that we some atoms on a region of $280\mu\text{m}$ while the remaining MOT atoms expand ballistically to a diameter of 2mm and the center cloud falls 8mm in the same time period.

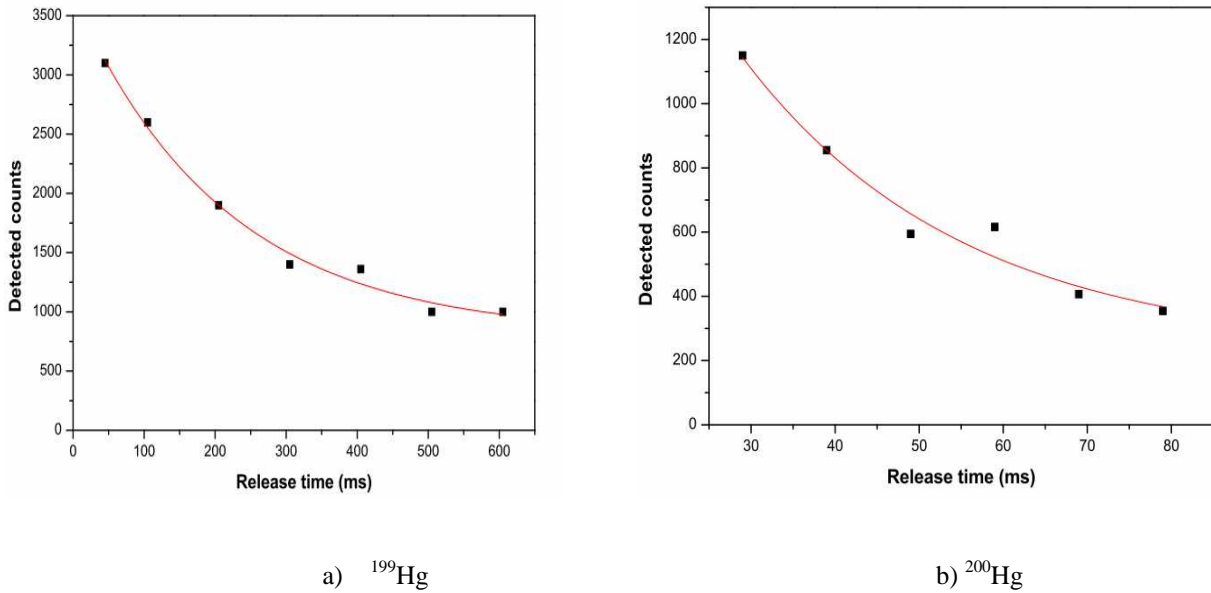


Fig.7. Lattice lifetime for the isotope ^{199}Hg and ^{200}Hg .

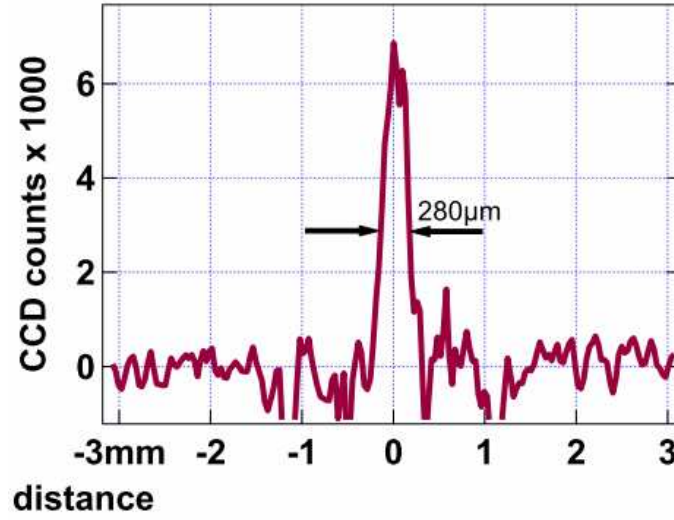


Fig.8. Cross section profile of the dipole trapped atoms after a 40 ms release from the MOT.

In order to further confirm trapping in the lattice, we apply a sinusoidal amplitude modulation on the lattice light during the detection delay in order to excite the longitudinal parametric resonance. Fig.9 shows the variation of the loaded fraction of atoms as a function of the excitation frequency.

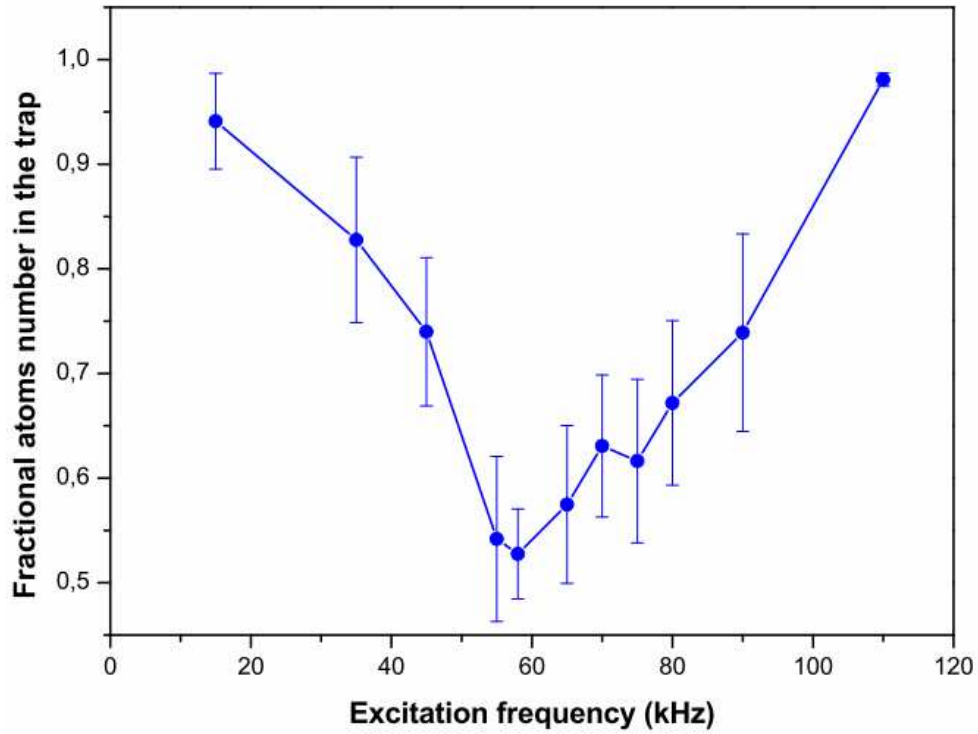


Fig. 9. Loaded atoms signal vs excitation frequency for a detection delay of 29 ms. This curve was measured for the ^{199}Hg isotope.

Based on this variation, the excitation frequency of the trap is in the range of 60 to 80 kHz, implying that the longitudinal trap frequency is at least 40 kHz. From expression (3) we find that the lattice circulating power is $\sim 2\text{W}$ (which is slightly lower than our initial estimation and which confirms that in addition to the sudden degradation of the internal power we have long term degradation). The corresponding trap depth is about $7E_R$.

CONCLUSIONS

We have implemented a CCD based atom detection system with high sensitivity, despite a number of challenges related to the use of mercury. For detecting lattice trapped atoms: 40 atoms produce a signal to noise ratio of one in one shot. We have developed and implemented an under-vacuum lattice cavity in conjunction with a MOT system. Atoms are transferred passively from the MOT to the lattice trap after shutting off the MOT fields. The low noise of the trap intensity insures that the trap does not suffer significantly from light induced parametric excitations; the cause of the lattice trap lifetime limitation is not yet clear.

We provide data indicating the first trapping of neutral mercury atoms in a 1D dipole lattice trap. A point to note is that we have observed lifetime in excess of 200 ms which is already sufficient for narrow line (Hertz level) spectroscopy of the clock transition.

This loading of the trap needs further augmentation so we can perform the spectroscopy of the clock transition in the Lamb-Dicke regime and experimentally determine the magic wavelength.

SYRTE is Unité Associée au CNRS (UMR8630) and a member of IFRAF cold atom network. This work is supported by IFRAF and CNES.

REFERENCES

- [1] T. Rosenband et al., Science 319, 1808 (2008)
- [2] Chou, C. W. et al., Phys. Rev. Lett. 104, 070802 (2010)
- [3] S. Bize et al., Phys. Rev. Lett. 90, 150802 (2003)
- [4] Blatt, S. et al., Phys. Rev. Lett. 100, 140801 (2008)
- [5] M. M. Boyd et al., Phys.Rev.Lett. 98, 083002 (2007)
- [6] A. D. Ludlow et al., Science 319, 1805 (2008)
- [3] H. Hachisu et al., Phys. Rev. Lett. 100, 053001 (2008)
- [4] S. Dawkins et al., Appl. Phys.B 99,41 (2009)
- [5] J. Millo et al., Phys. Rev. A 79, 053829 (2009)
- [6] M. Petersen et al., Phys. Rev. Lett. 101, 183004 (2008)
- [7] H. Katori et al., Phys.Rev.Lett. 91, 173005 (2003)
- [8] M. E. Gehm et al., Phys.Rev.A. 58, 3914 (1998)